

BLOOD FLOW IN THE LUNG*†

R. COLLINS and J. A. MACCARIO

University of Compiègne, BP 233, 60206 Compiègne, France

Abstract – Pulmonary hemodynamics is studied in terms of the quasi one-dimensional unsteady nonlinear fluid flow equations which are applied to the 40-odd generations of branched arterial, capillary and venous distensible vessel segments making up the four lobes of the complete lung. An idealized pressure–area “tube law” is introduced which provides for varying degrees of vessel collapse. The model predictions agree well with experimental measurements of flow transmission as a function of pulsatile frequency. Pulmonary response is represented schematically in terms of an influence diagram. Pressure pulses are shown to increase in amplitude in the early arterial segments, with the greatest drop occurring across the capillary bed.

1. INTRODUCTION

The lung constitutes a highly complex and self-regulating system for oxygenating man's blood and removing its waste materials. It is at the alveolar level that the respiratory and circulatory functions interact and the important exchange processes occur. Much research has been done on both aspects of pulmonary function by physiologists, medical clinicians and applied mathematicians. It is evident from this work that mechanical principles play a very important role. Neural control is nonetheless present, although less prominent than in the systemic circulation. Its direct effect may enter, however, through a readjustment of the mechanical variables of the system.

It is particularly the circulatory aspects of pulmonary function which are of concern in the present investigation. We address ourselves here to the general question of how the lung might adapt to external influences, caused for example, by cardiac dysfunction (mitral stenosis, left-to-right shunts), vascular obstructions (emboli transported to the lungs from the systemic veins), changes in altitude (alterations in alveolar pressure in mountain-climbers and deep-sea divers) and physical work and exercise. A good quantitative understanding of pulmonary response is still lacking to this date, although a number of very imaginative experiments have been undertaken to document this behaviour. Less work has been done on the unification of this data in the form of a global quantitative model of the complete circulatory system of the lung on the basis of classical mechanical principles.

Some may be of the opinion that such an undertaking is premature. Indeed, very little detailed and utilizable information is available for the material properties on which the results of such an analysis must depend. Direct measurements of *in vivo* dimensions and mechanical properties of the intricate branching network have been accomplished only for

the main pulmonary artery and its early branches. Beyond, this point, the calibre of the vessels rapidly diminishes. Nor can the vascular beds be laid out in thin sheets so that their *in-vivo* behaviour may be examined dynamically under a microscope. The anatomy of the rabbit's ear may readily lend itself to such experimentation, but the lung is highly three-dimensional in structure.

Partial circumvention of this difficulty is possible by injection into the blood-stream of a substance which is at first convected and then solidifies within the blood vessels, hopefully without changing their dimensions. Measurements are then made directly on the cast of the pulmonary tree of the sacrificed animal.

Similar difficulties apply to measurements of transmural pressure beyond the first and last few generations. Reliance on venous “wedge” pressures, obtained by occluding the vessel to the point of arresting the flow, is less than satisfying, for some doubt always remains about their correct interpretation. Flow measurements in the interior of the lung have been carried out recording the radiation from gaseous radioactive tracers, such as xenon-133, which may be injected into the blood-stream and detected by an external counter. One thus obtains an integrated measure across a slice of the lung.

In spite of this somewhat pessimistic picture, useful estimates have been made in the intermediate regions of the lung, which serve as a starting point for a mathematical analysis. One may cite the now classical studies of lung morphology by Weibel (1963) and the more recent findings of Cummings *et al.* (1969). However the results of Wiener *et al.* (1966) offer the considerable advantage of accompanying their estimations of vessel dimensions by values of the corresponding vessel compliances.

Useful measurements of pressure and blood flow in different regions of the lung under varying conditions of flow pulsatility have been published by Attinger (1963), West *et al.* (1964) and Maloney *et al.* (1968).

Mathematical modelling of the pulmonary circulation has been attempted at various levels of detail. Global response has been simulated by a great many investigators (for example, Rideout and Katra, 1969)

* Received 12 September 1978.

† Reprints from Prof. R. Collins, 130 Blvd des Etats-Unis, 60200 Compiègne, France.

on the basis of the analogy of the linearized equations of motion with an electrical transmission line. The notions of resistance or impedance connected with this simplified formulation have found great popularity amongst physiologists who find such physically intuitive concepts useful in their quest for an understanding of the fundamental underlying mechanisms of pulmonary behaviour. One must nonetheless proceed with caution in interpreting the results of such formulations which often do not deal adequately with important intrinsically nonlinear characteristics such as wave steepening and hence the growth of pressure amplitudes observed along the arterial segments of the circulatory system.

A more realistic approach requires retaining the important nonlinear inertial terms in the fluid equations of motion. The resulting system is of second order, and hyperbolic in character, provided that the transmural pressure is considered to be a function of local cross-sectional area only. It may be solved numerically by finite differences or by the method of characteristics. The latter technique has been employed by Anliker *et al.* (1971) for the systemic circulation. Since it is difficult to include the complete systemic circulatory system in such calculations, provision must be made for outflows from the model system, by means of continuous or distributed sinks. A similar procedure has been adopted here, with the added advantage that the complete pulmonary anatomy may be included in the model, thus obviating the need for such pre-specified sink terms.

It has long been recognized that distensible blood vessels may collapse, at least partially, under physiological flow conditions. Such vessels become approximately elliptical in cross-section, the ratio of major-to-minor axes ranging in dogs from 1.25 in the main pulmonary artery to 1.91 within the next five arterial generations. These measurements of Attinger (1963) correspond to equivalent cross-sectional area ratios of 0.72–0.82 between elliptic and circular configurations. Attinger concludes that these ratios at the major branch points are considerably less than those postulated for optimal energy transfer. One is thus led to surmise that collapsible vessels, which disadvantage the efficient transmission of energy, may be playing another role, for which that is the price.

The suggestion that the purpose of collapsible pulmonary capillaries may be to control the flow, as a "Starling" resistor, was first introduced by Permutt *et al.* (1962). They regarded such collapsible vessels, subjected to upstream arterial, downstream venous and surrounding alveolar pressures, as sensitive sluiceways which open or close in response to these three forces. West *et al.* (1964) have extended this idea to define three control-zones in the lung:

upper lung: zone 1: arterial < alveolar > venous pressures – totally collapsed
intermediate lung: zone 2: arterial > alveolar > venous pressures – collapsed at distal end

lower lung: zone 3: arterial > venous > alveolar pressures – fully open.

At the bottom of the lung (zone 3) where the pulmonary vessels are completely open, the flow rate depends classically upon the arterial and venous pressure difference. However the situation is rather novel in the intermediate zone 2, where the flow rate is controlled by the arterial–alveolar pressure difference, independently of the value of the venous pressure, which is less than the alveolar pressure. Permutt refers to this as the "waterfall effect", an obvious and graphic analogy which has been generally confirmed by experiment.

However, the model must be tempered somewhat by realizing that zones 1, 2 and 3 merge gradually into one another, during the interplay of reflecting pressure waves within a branching system of distensible tubes of varying compliance. Furthermore, a "surfactant" alveolar lining which lowers surface tension, may keep capillaries open even for slightly negative values of the transmural pressure (Bruderman *et al.*, 1964).

A rigorous analysis of the dynamics of collapsible tubes has not yet appeared in the literature, although a first attempt in this direction has been made by Collins (1978). A recent steady-state analysis by Shapiro (1977) is of considerable interest, although the "sonic" type singularities inherent in that solution may possibly not be appropriate to pulsatile flows which appear to be free of the restrictive compatibility conditions invoked for steady flow.

We will conclude this brief and not exhaustive summary of previously proposed mathematical models of the pulmonary circulation by mentioning the very interesting "sheet flow" concept introduced by Fung and Sobin (1969) to describe blood flow in the pulmonary capillary bed. The steady-state Hele-Shaw flow about the "posts" enclosed in the "sandwich" model of the idealized pulmonary vascular bed depends upon maintenance of very low flow Reynolds numbers for the absence of non-stationary wall flutter effects.

The important question here is whether capillary vessels open and close in response to the instantaneous values of transmural pressure alone, or whether there exists a spectrum of finite opening times for collapsible vessels, as proposed by Maloney *et al.* (1968a). From the more general coupled solution of the fluid and wall equations (Tedgui and Collins, 1978), in lieu of the usual practice of introducing a pre-specified pressure–area law, it would appear that the Reynolds number may not constitute the only criterion by which dynamic effects are to be estimated. In addition, the residual axial wall tension and the distribution of longitudinal wall curvature may cause the vessel to "vibrate" in a manner reminiscent of a stretched violin string. But this complex behaviour will not be developed further here.

In the following sections, the morphology of the lung will be modelled in a discretized form, and flow

predictions based on it in conjunction with a non-linear method of characteristics solution described in the subsequent section will be tested against the results of Wiener *et al.* (1966) for the pulmonary circulation of the dog. The validated mathematical model will then be used to investigate the dynamics of flow transmission in the lung at different frequencies, and the results will be compared with the measurements of Maloney *et al.* (1968).

2. MORPHOLOGY OF THE PULMONARY CIRCULATION

A variety of different casting techniques has been reported for the measurement of the large and fine structures of the irregular branching network of pulmonary arterial and venous vessels. A typical procedure (Cumming *et al.*, 1970) may involve fixing the inflated lungs with liquid formalin (so as to eliminate gravitational effects), injecting a thermosetting resin and finally dissolving the surrounding lung tissue with hydrochloric acid (less viscous liquids are required to permeate the finer vessels). The lengths and diameters of the larger vessels (> 2 mm) may be measured directly with calipers, while the dimensions of the finer and more fragile segments (40 μm ~ 1 mm) of the cast may be determined from corresponding photographs using a scanning electron microscope. For the latter, sampling techniques must suffice to

gauge the mean dimensions of the approximately 10 μm vessels supplying each of the estimated 3 × 10⁸ alveolar syncytia.

The left side of the lung is of smaller volume than the right, probably as a result of the space occupied by the heart. The estimated left to right volume ratio of 0.82 (Cumming *et al.*, 1970) thus gives rise to some asymmetry in the branching ratios, as the two sides are perfused from the main pulmonary artery common to both. Much of the difficulty in characterizing the morphology of the pulmonary circulation has its origin in this asymmetry, and in the irregularity of the branching daughter vessels.

For the purposes of our analysis of blood flow in the lung, four properties are of particular interest: the general architecture of the lung, the distribution of number, lengths and cross-sections of its branching vessels, the mechanical constitutive relations (e.g. pressure-area law) of these vessels, and finally the pressure and flow profiles at the proximal and distal extremities of the lung. Although statistical and sampling difficulties may well cast doubts on the precision obtainable, only the data of Wiener *et al.* (1966) for the dog lung appear to embrace all four of the required categories for a given network.

Their representation of the lung in terms of 4 lobes is depicted in Fig. 1, and incorporates an averaged (although structurally incorrect) system of regular dichotomous branching: whereas Cumming *et al.*

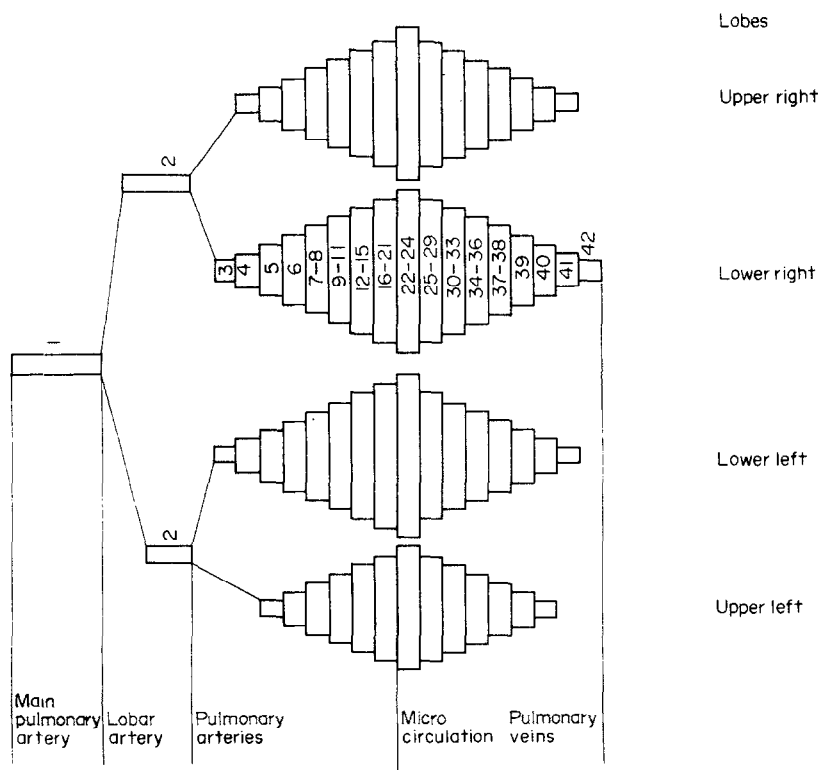


Fig. 1. Discretized 4-lobe model of lung with generation numbers corresponding to lower right lobe (cf. Table 1).

Table 1. Idealized segments of equivalent lower right lobe on basis of Wiener *et al.* (1966) data

Generation number	Wiener data for lower right lobe			Idealized segments of equivalent conduit					
	G	Length $L(\text{cm} \times 10^{-1})$	Cross-section $S(\text{cm}^2)$	Compliance $\alpha(\text{cm}^4/\text{dyn} \times 10^6)$	Length $L(\text{cm} \times 10^{-1})$	Cross-section $S(\text{cm}^2)$	Compliance $\alpha(\text{cm}^4/\text{dyn} \times 10^6)$	Number of vessels N	
Pulmonary arterial segments	3	16.85	0.3800	10.4110	16.85	0.3800	10.4110	1	
	4	13.65	0.4827	11.785	13.65	0.4827	11.785	2	
	5	11.06	0.6132	13.339	11.06	0.6132	13.339	4	
	6	8.956	0.7790	15.097	8.956	0.7790	15.097	8	
	7	7.255	0.9896	17.092	13.1320	1.1093	18.0975	23	
	8	5.877	1.257	19.339					
	9	4.761	1.597	21.907	11.7410	1.9996	24.4898	130	
	10	3.856	2.029	24.789					
	11	3.124	2.577	28.057					
	12	2.530	3.274	31.771					
	13	2.050	4.159	35.962	7.5850	4.5623	37.3947	14.10 ²	
	14	1.660	5.283	40.701					
	15	1.345	6.711	46.076	4.1160	14.5623	67.4230	46.10 ³	
	16	1.090	8.525	52.141					
	17	0.883	10.889	59.035					
	18	0.715	13.760	68.829					
	19	0.579	17.475	75.655					
	20	0.469	22.20	85.615					
	21	0.380	28.20	96.907					
	Capillary bed	22	0.740	71.40	87.073	2.2100	159.92	230.23	29.10 ⁶
		23	0.810	290.60	373.04				
24		0.660	98.80	214.48					
25		0.445	32.70	218.66					
Pulmonary venous segments	26	0.5493	25.54	180.60	3.5439	19.1150	152.81	66.10 ³	
	27	0.6783	19.95	159.26					
	28	0.8373	15.58	135.89					
	29	1.0338	12.17	115.98	7.1986	6.3882	76.033	29.10 ²	
	30	1.2763	9.506	98.979					
	31	1.5756	7.424	84.460					
	32	1.9452	5.799	72.082					
	33	2.4015	4.529	61.509					
	34	2.9648	3.538	52.500					
	35	3.6603	2.7631	44.799	11.1440	2.7240	44.196	260	
	36	4.5189	2.1582	38.232					
	37	5.5789	1.6887	32.626	12.4664	1.4818	29.984	45	
	38	6.8875	1.3166	27.843					
	39	8.5031	1.0284	23.761	8.5031	1.0284	23.761	16	
	40	10.4976	0.8032	20.276	10.4976	0.8032	20.276	8	
	41	12.9600	0.6274	17.305	12.9600	0.6274	17.305	4	
	42	16.0000	0.4900	14.767	16.0000	0.4900	14.767	2	

Main arterial segments: pulmonary artery: $L = 2.3$, $S = 1.33$, $\alpha = 40.923 \times 10^6$;
left lobar artery: $L = 1.4$, $S = 0.60$, $\alpha = 18.462 \times 10^6$;
right lobar artery: $L = 2.08$, $S = 0.60$, $\alpha = 18.462 \times 10^6$.

(1970) suggest that the most likely configuration is characterized by a branching ratio (number of daughter vessels arising on average from each parent) of 3.26 for the right lung and 3.50 for the left. In order to formulate an efficient computational procedure which still retains the salient mechanical features of the pulmonary circulation, successive groups of comparable generations (i.e. of similar lengths and cross-sections) were gathered into equivalent segments of a single conduit, one for each of the 4 lobes. Only the first and last few generations of the larger pulmonary

arterial and venous vessels respectively were maintained in their original configurations, while the complete vascular bed was absorbed into an individual segment of equivalent total volume. Table 1 shows a typical restructuring of the Wiener data for the lower right lobe in terms of the lengths L , cross-sectional areas S , compliances α and number of vessels N comprising each idealized segment of the equivalent tube. Segments in the left lung were taken to be 30% narrower than in their right-hand counterpart, rather than the 50% differences occasionally evident in the

data of Wiener *et al.* (1966). It will be shown later that the distal pressure and flow profiles in the pulmonary vein are not overly sensitive to such anomalies in an individual lobe, as they are largely compensated by confluent flows in the remainder of the pulmonary circulation. In view of the limitations of this observed pulmonary response and the rather imprecise nature of the morphological data currently available, the presently proposed discretized lobular configuration would appear justifiable.

The distribution of vessel lengths and cross-sections from one generation to the next may be characterized reasonably well in the form of a geometric progression. Attinger (1963) proposes common ratios for the arterial and venous segments of the order of 0.8 and 1/0.8, respectively, while the variation of the cumulative arterial vessel cross-sections by generation has been characterized by common ratios ranging from 1.1 to 1.28 by Caro *et al.* (1965), Cumming *et al.* (1969) and Wiener *et al.* (1966). It is most important that the final equivalent "tube" configuration so developed does not contain abrupt changes in cross-sectional area or large divergence angles which could precipitate a spurious separation of the flow.

Of the remaining two aspects of the characterization of the model lung, the pressure-area law is described in the next section, followed by the pressure and flow profiles required as boundary conditions to the numerical computation.

3. MATHEMATICAL FORMULATION

Each of the four pulmonary lobes is discretized in the form of a single equivalent elastic conduit of non-uniform cross-section, by grouping successive generations of branching vessels into uniform segments as described in the previous section. Care must be taken to avoid spurious flow separation between adjoining segments by limiting the axial variation of cross-sectional areas in the idealized model. With this provision, the discretized morphology can lead to a considerable economy in computational effort.

3.1 Governing equations of motion

The quasi one-dimensional unsteady equations of motion for flow of a viscous incompressible fluid in a deformable conduit of varying cross-section S may be expressed as

$$\frac{\partial S}{\partial t} + \frac{\partial(vS)}{\partial x} = 0, \quad (3.1)$$

$$\frac{\partial v}{\partial t} + \frac{\partial}{\partial x} \left(\frac{v^2}{2} + \frac{p}{\rho} \right) - F = 0, \quad (3.2)$$

where v is the blood velocity averaged over the local cross-section, p , the locally-averaged transmural pressure, ρ , the blood density, and F , the friction factor accounting for viscous drag between the blood and the vessel wall. Clearly this friction factor must be based upon the true vessel dimensions, and not upon the size

of the equivalent lumped conduit.

The one-dimensional friction factor F is defined in terms of the shear stress τ at the wall as

$$F = \frac{2}{\rho r} \tau, \quad \text{with } \tau = C_f \cdot \frac{1}{2} \rho v^2 \text{Re}^{-m}, \quad (3.3)$$

where Re is the Reynolds number based on the true vessel radius r . For the laminar flow considered here, the parameters C_f (skin friction) and m take on the values (Kivity and Collins, 1974) $m = 1$, $C_f = 8$.

In terms of the true vessel cross-section $A (= \pi r^2)$, the friction factor is expressed as

$$F = - \frac{8\pi}{A} \frac{\mu}{\rho} v, \quad (3.4)$$

and acts in a direction opposing fluid motion. If at a particular station, N such vessels of cross-section A have been combined to form the corresponding equivalent conduit of cross-section S , then F may be re-expressed in terms of the equivalent tube as

$$F = -8\pi \frac{N}{S} \frac{\mu}{\rho} v. \quad (3.5)$$

As particular vessels approach a progressively collapsed state during the cardiac cycle, relation (3.4) becomes modified toward an inverse quadratic law $F \sim 1/A^2$. However, since only a fraction of the true vessels making up the "equivalent" tube configuration will be grossly non-circular at any instant, relation (3.5) still remains a reasonable representation of the friction factor for the quasi one-dimensional flows studied here.

For a system of elastic vessels, the transmural pressure can be expressed as a function of the single argument S . (Within this same condition, an approximate provision may be made for vessel collapse in the event of negative transmural pressures). The resulting system of second-order linear differential equations is hyperbolic and may be re-cast into characteristic form

$$dp \pm \rho c dv = \pm \Gamma \frac{v}{S} \quad (3.6)$$

along the respective characteristic directions

$$\frac{dx}{dt} = v \pm c, \quad (3.7)$$

where the signal propagation velocity

$$c^2 = \frac{S}{\rho} \frac{\partial S}{\partial p} \quad (3.8)$$

with

$$\Gamma \equiv \rho c 8\pi N \frac{\mu}{\rho} dt.$$

It is noted here that a more generalized (viscoelastic) pressure-area law for the equivalent conduit would entrain higher derivatives, invalidating a solution by the method of characteristics. These points have

been discussed in some detail by Anliker *et al.* (1971) and Collins (1978). In the latter work, it has been demonstrated that in the partially-collapsed state ($p < 0$), the transverse component of the axial tension may play an important role in opposing complete closure of the tube, and that this force component is proportional to the local longitudinal curvature. The first and second derivatives which then enter into the pressure-area relation would upset the second-order character of the present system. For this reason, an approximate, but still realistic treatment, valid for limited degrees of collapse (see Shapiro, 1977), is adopted. For $S \geq S_0$ (the just distended cross-sectional area S_0 corresponding to $p = 0$)

$$S = S_0 + \alpha p, \tag{3.9}$$

where α is the average compliance of the tube segment, while for $S \leq S_0$, (partially collapsed state, for which $p \leq 0$)

$$S = S_0 \left(\frac{-P}{K_p} \right)^{-2.3} \quad \text{for} \quad \frac{P}{K_p} < -1.5$$

and (3.10)

$$S = S_0 \left[0.017 \left(\frac{P}{K_p} \right)^3 - 0.069 \left(\frac{P}{K_p} \right)^2 + 0.015 \frac{P}{K_p} + 1 \right]$$

for $-1.5 < \frac{P}{K_p} < 0$,

where K_p is a proportionality factor.

The introduction of the third order polynomial allows one to bridge the gap between the similarity $p^{-2.3}$ law in the region of collapse and the linear αp law in the inflated region without incurring a discontinuity in the derivative $\partial S / \partial p$ at the point of transition $S = S_0$.

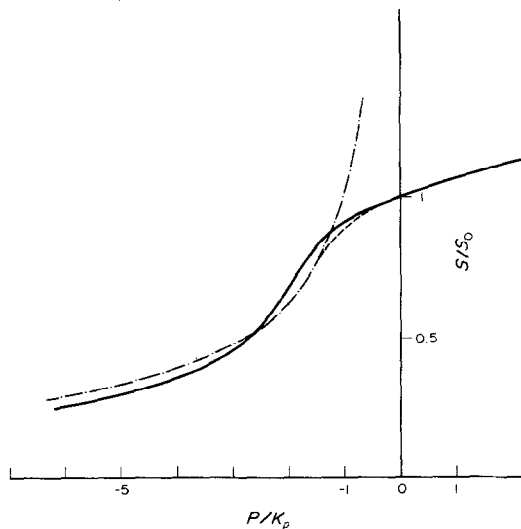


Fig. 2. Pressure-area relation for pulmonary vessels.
 — Experiments (Shapiro 1977).
 - - - Similarity law $(P/K_p)^{-2/3}$.
 Third order polynomial bridge.

The continuous pressure-area relation (3.10) is sketched in Fig. 2 along with the corresponding experimental curve and the approximation of Shapiro (1977). The portion corresponding to negative transmural pressures will be invoked selectively over certain portions of the pulmonary network as a means of assessing quantitatively the as yet not fully understood contribution of vessel collapse to pulse transmission in the lung.

The vessel wall compliance α is seen from Table 1 to increase as a geometric progression with common ratio of approximately 1.16 as one proceeds along the roughly 20 generations of arterial branchings toward the capillary bed. This does not necessarily imply, however, that the corresponding modulus of elasticity E varies inversely in the same proportions, as the cumulative cross-sectional area increases with a common ratio of about 1.28 (with a constant radius-to-wall thickness ratio R/h of 10). The net effect on the elastic modulus $E \sim S/\alpha$ is an increase (progressive "stiffening" along the arterial segments), with a common ratio of approximately 1.1 as one approaches the vascular bed. Milnor *et al.* (1969) draw attention to the possibility that arterial stiffening may be associated with some aspects of pulmonary hypertension.

The compatible boundary conditions are those of specified velocity or pressure at the network ends (held at fixed cross-section) and continuity of pressure and mass flow at the internal branch points.

3.2 Difference equations

The three equations (3.6, 3.9 and 3.10) in the three hodograph variables p, v and S may be integrated in the $x-t$ plane by a method of characteristics progressing along fixed increments in time (Fig. 3). Nominally uniform initial conditions are specified, and the calculation evolves very rapidly toward a completely cyclic

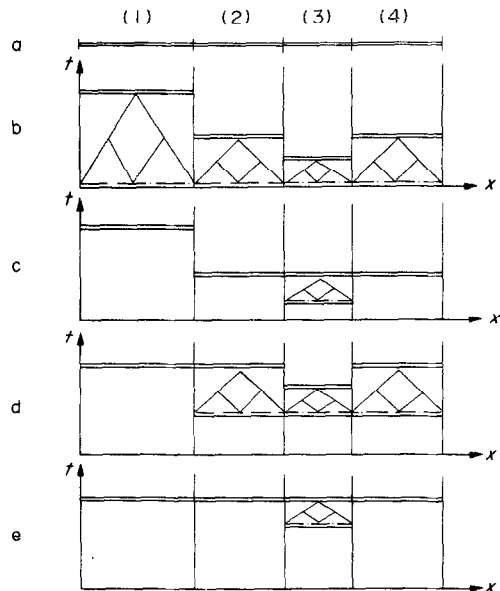


Fig. 3. Computational network in $x-t$ plane.

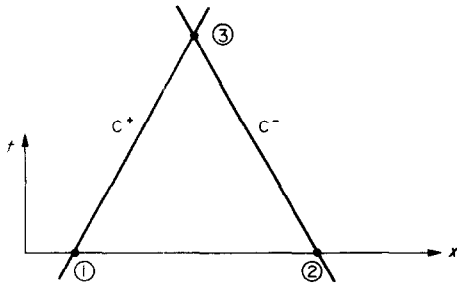


Fig. 4. Characteristics net for typical interior points.

behaviour, corresponding to pulsatile flow at different cardiac frequencies.

Slightly different numerical procedures are adopted for the bifurcation points within the branching network of vessels.

3.2.1 *Interior points.* The solution at a new time $t_3 (= t + \Delta t)$ and position x_3 is computed from the known solution at time $t (= t_1 = t_2)$ by determining two points x_1 and x_2 (by iteration) whose characteristics intersect 3 at the pre-specified time increment Δt (Fig. 4).

For these three points, equation (3.6) become

$$(p_3 - p_1) + \rho c_1(v_3 - v_1) = -\Gamma \frac{v_3}{S_3} \quad (3.11)$$

$$(p_3 - p_2) - \rho c_2(v_3 - v_2) = +\Gamma \frac{v_3}{S_3}$$

In terms of $T_1 = p_1 + \rho c_1 v_1$ and $T_2 = p_2 - \rho c_2 v_2$, and after elimination of v_3 from (3.11) the pressure at point 3 becomes

$$p_3 = \frac{T_1 \left(\rho c_2 + \frac{\Gamma}{S_3} \right) + T_2 \left(\rho c_1 + \frac{\Gamma}{S_3} \right)}{\rho c_2 + \rho c_1 + 2\Gamma/S_3} \quad (3.12)$$

which may be solved iteratively, starting from an initial estimate of p_3 and use of (3.9) or (3.10). Knowing the converged value of S_3 , the solution for v_3 is obtained directly by eliminating p_3 from equations (3.11) in the form

$$v_3 = \frac{T_1 - T_2}{\rho c_1 + \rho c_2 + 2\Gamma/S_3} \quad (3.13)$$

3.2.2 *Junction points.* At the junction between segments, one may encounter a jump in the cross-sectional area, to which the solution is very sensitive. It is partly for this reason that S_3 was introduced into the right-hand members of the difference equations (3.11). One must distinguish here between stations distal (') and proximal (") to the junction (Fig. 5).

In terms of the C^+ characteristic emanating from the proximal segment a, and the C^- characteristic from the distal segment b, the difference relations take on the form:

$$(p'_3 - p_1) + \rho c_1(v'_3 - v_1) = -\Gamma_1 \frac{v'_3}{S_3}$$

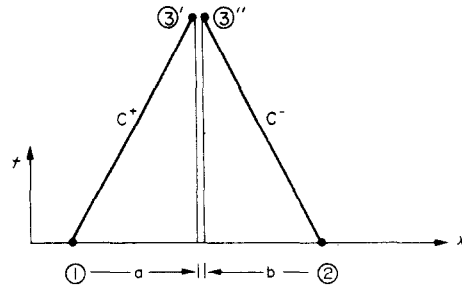


Fig. 5. Characteristics net at junction between two vessel segments.

$$(p''_3 - p_1) + \rho c_2(v''_3 - v_2) = \Gamma_2 \frac{v''_3}{S_3} \quad (3.14)$$

Continuity of pressure and flow rate are expressed respectively as

$$p'_3 = p''_3 \quad (3.15)$$

and

$$v_3 \cdot S_3 = v_3 \cdot S_3 \quad (3.16)$$

It is evident from (3.16) that a discontinuity in cross-sectional area at the junction between two discretized segments will lead to a similar jump in the flow velocity. Although such discontinuities indeed occur at physiological bifurcations of individual blood vessels, the effect may however be amplified in the idealized conduit segments, in which several generations have been combined.

The solution of the system of difference equations at a junction point follows in much the same manner as described above for interior points, without any particular difficulty.

3.2.3 *Ordering of computations.* The slope of the individual characteristic curves varies by a factor of approximately five within the forty-odd generations of arterial and venous branchings, attaining its highest values within the capillary bed. This feature considerably complicates the internal "accounting" system, by which stations within and at the extremities of vessel segments must be identified in space and time. In particular, pressure and flow rates at the junctions of adjoining segments must be matched at identical instants of time.

A system of fixed-time increments is most suitable for satisfying these requirements, and is achieved by transposing flow values to the desired time levels through interpolation along the respective characteristic directions. Since the characteristic network in certain regions advances five times more rapidly than in others, the "valleys" thus created in the computational net must be progressively filled in the slower wave-speed regions, before advancing the rapid zones.

Without entering into the tedious details of the programming necessary to advance the flow variables in time throughout the complete pulmonary network, one may summarize the ordered procedure as in Fig. 3.

As a result of the repeated interpolations required to transpose flow variables calculated at the intersections

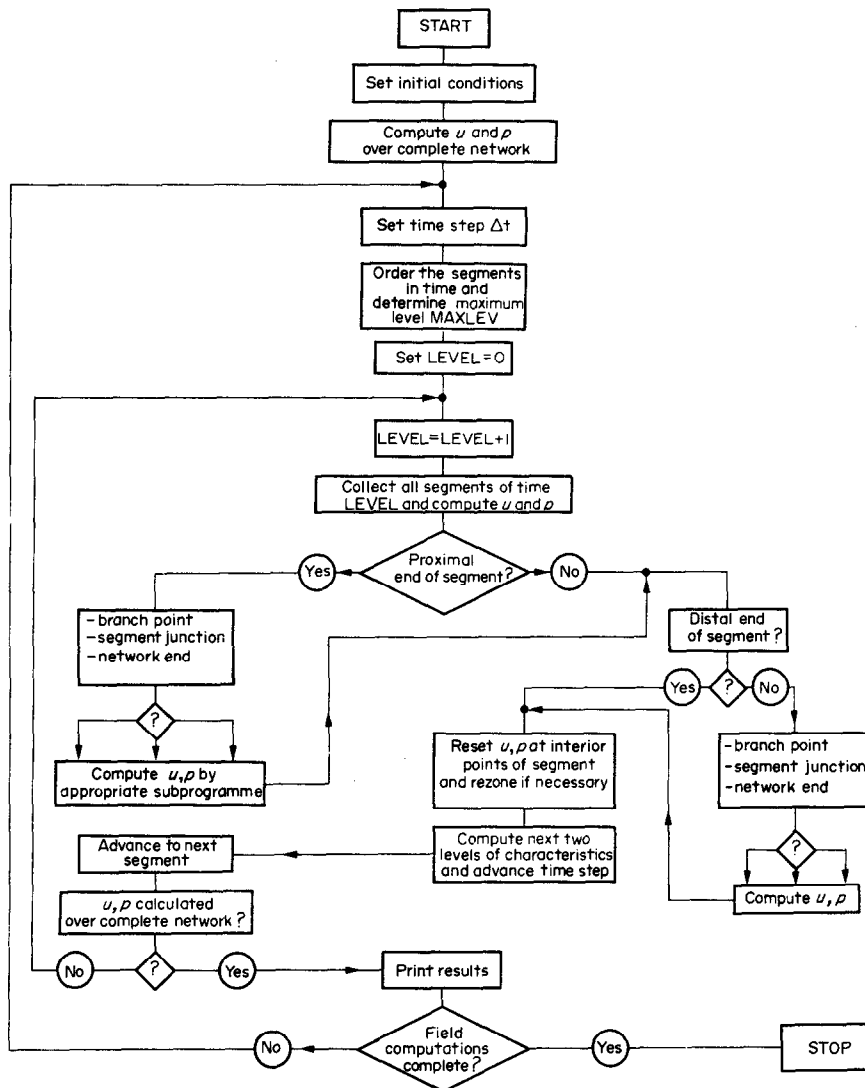


Fig. 6. Computational flow chart.

of characteristic curves to the desired fixed-time intervals, the computational net may progressively skew to the left or right. A rezoning in the spatial coordinate becomes useful when the ratio between the largest and small Δx increments exceeds a value of two. A detailed flow diagram representing the overall programmed computational procedures appears in Fig. 6.

4. VALIDATION OF THE MODEL

Wiener *et al.* (1966) furnish pressure and flow profiles which have been measured at the proximal and distal extremities of the lung, and calculated (by linear theory) at intermediate generations. A judicious choice must be made in validating the numerical predictions of the present model with those data, which are not fully satisfactory for this purpose. In effect, the distal flow profiles (Fig. 7) reported by Wiener *et al.* (1966)

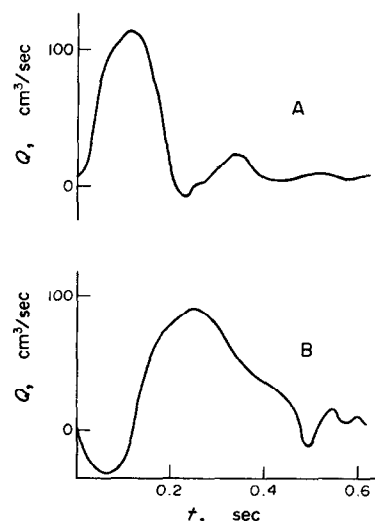


Fig. 7. Measured flow profiles (Wiener *et al.*, 1966).
A: pulmonary artery.
B: left atrium.

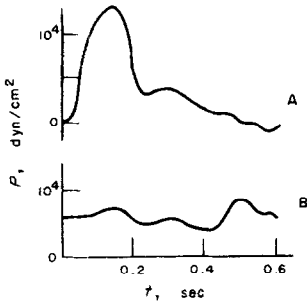


Fig. 8. Measured intra-luminal pressure profiles (Wiener *et al.*, 1966).

A: right ventricle.
B: left atrium.

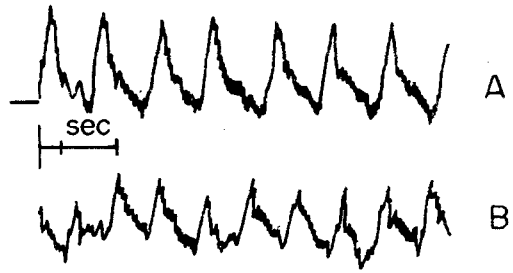


Fig. 9. Experimental recordings at outlet from lung (Morkin *et al.*, 1965).

A: flow rate in the "small" veins.
B: distal venous pressure.

Table 2. Characteristics of 14 cases computed for comparison with flow transmission measurements of Maloney *et al.* (1968b)

Pulsatile frequency (H_2) Operating Conditions	0.5	1	2	3	5
	No collapse and normal compliance 	Case 1	Case 2 (fig 12)	Case 3	Case 4 (fig 13)
With collapse (pre-cap → atrium) 	Case 8	Case 9 (fig 15)	Case 10	Case 11 (fig 16)	
			Case 12 10,000 identical with fig 12		Case 13 reserved flow (fig. 17)
				Case 14 collapse restricted to capillary bed	

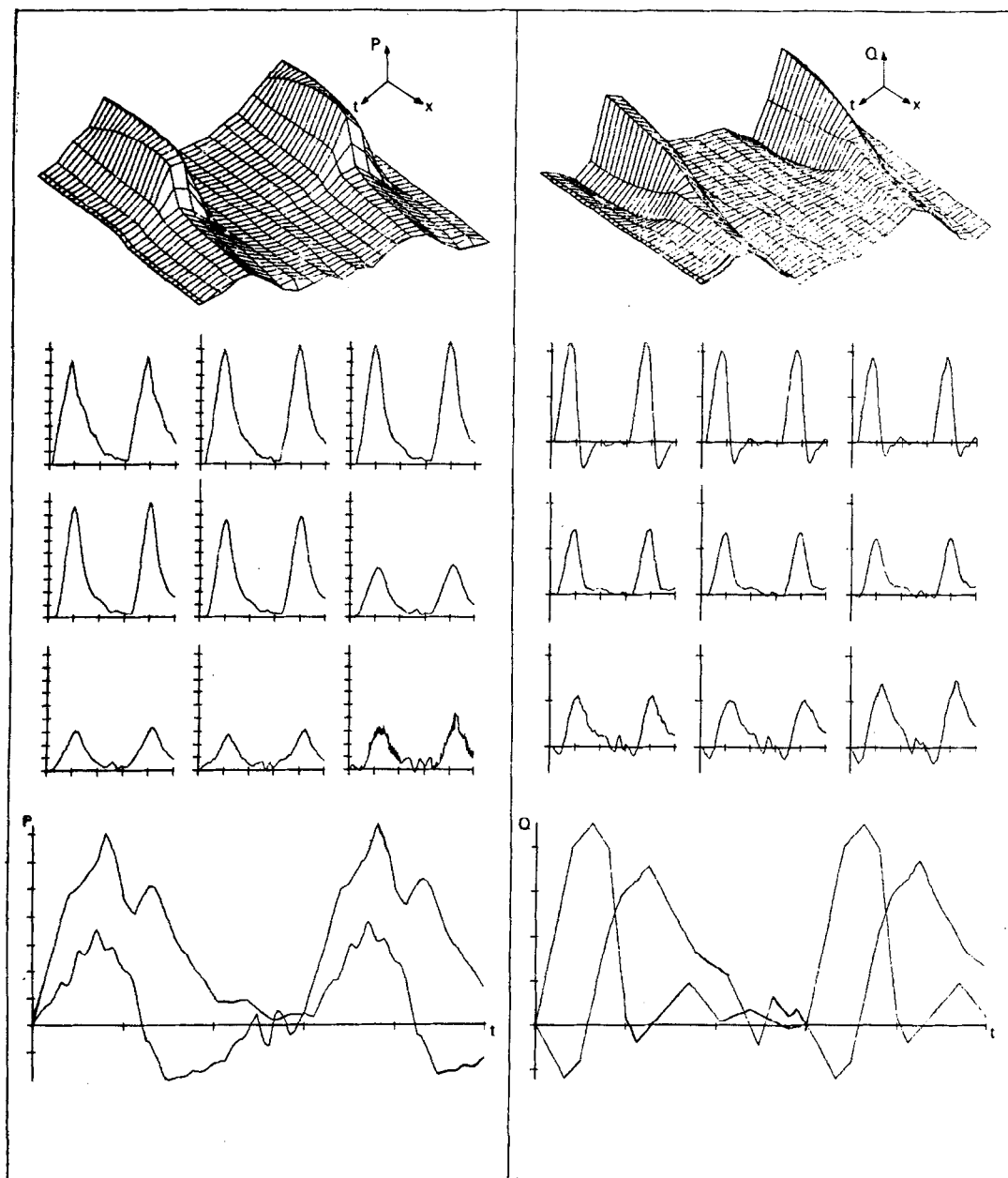


Fig. 10. Computed pulmonary pressure and flow fields for validation with measured data of Wiener *et al.* (1966). Explanation of corresponding stations is provided in Section 5.

represent the combined output from the four lobes. We have assigned to each lobe a fraction of the total outflow in proportion to the distal venous cross-section corresponding to each respective lobe. Furthermore, Wiener *et al.* (1966) report absolute values of the intra-luminal pressures (Fig. 8), but neglect to specify the extravascular levels which would permit one to ascertain the required transmural pressures. The pressure profiles for the pulmonary vein are

surprisingly free of the local oscillations (Fig. 9) associated with the corresponding data of Morkin *et al.* (1965), and one may suspect that the pulmonary venous pressures reported by Wiener *et al.* (1966) would better represent catheter measurements at a position closer to the left atrium, where a certain degree of damping would have taken place. It must further be assumed that the morphological data of Wiener *et al.* (1966) (Table 1) refer to the right lower

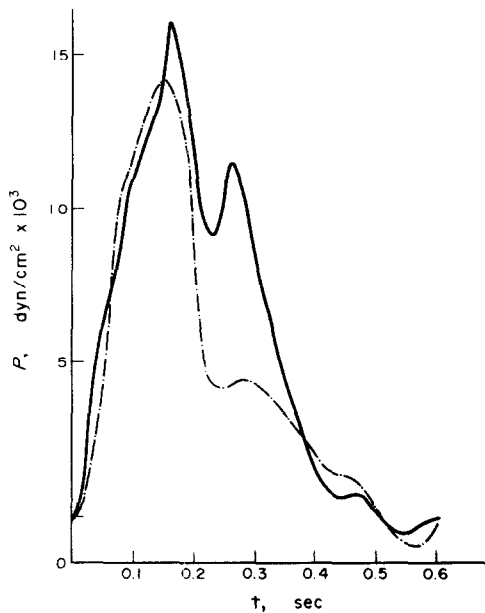


Fig. 11. Computed proximal pressure profile (solid curve) using measured flow boundary conditions of Wiener *et al.* (1966) and comparison with their measured proximal pressure profile (dashed curve).

lobe, on the basis of the associated number of generations reported. For these reasons, it is not completely clear, for the purposes of validation, whether more confidence should be placed in the pressure boundary conditions, from which the flow profiles may be calculated and compared, or vice versa.

A number of cases have been computed corresponding to both these alternatives, for each of which the relative roles played by fluid viscosity and vessel wall collapse have been assessed. One such comparison is given in Fig. 10, for which the reduced vessel calibre of Wiener *et al.* (1966) was preserved. The boundary conditions imposed at the proximal and distal ends were those of flow rate, proportioned to the lower right lobe, and modified by the measurements of Morkin *et al.* (1965). The computed pressure profiles which result are seen to be in good qualitative agreement with the measurements of Wiener *et al.* (1966), once converted to their transmural counterpart (Fig. 11).

The rôle of fluid viscosity (taken as 4 centipoise) appears to be essential in these calculations. In the absence of viscosity, incoherent non-cyclic oscillations develop in the calculation, partly as a result of the cumulative undamped effects of wave reflections at the junctions between adjoining vessel segments.

The influence of vessel collapse cannot be adequately evaluated, however, for the Wiener *et al.* (1966) data from which one deduces transmural pressure levels which remain essentially positive. Testing of the provisions for vessel collapse in the present model must therefore be reserved for the flow distribution experiments of Maloney *et al.* (1968), which will be discussed in the following section.

5. COMPUTATIONAL RESULTS

Following the validation in the previous section of the mathematical model by comparison with the published results of Wiener *et al.* (1966), we are now in a position to examine the behaviour of the solution in response to selected variations in the following four factors: (a) pulsatile frequency (at proximal end), (b) vessel wall compliance, (c) extent of vessel collapsibility and (d) absolute pressure level and effect of reversal of pressure gradient.

Fourteen complete cases have been computed for the pressure and flow variations in the lower right lobe (typical of the four pulmonary lobes) and may be summarized as in Table 2. Of these, six have been selected to illustrate some physical characteristics of the pulmonary circulation.

In these numerical results, the boundary conditions selected conform very closely with those applied in the experiments of Maloney *et al.* (1968). The distal end is maintained at a constant pressure level, while a sinusoidal pressure variation is applied at the proximal extremity at frequencies varying from 0 to 5 Hz. Complete pressure and velocity fields are then computed. Slight incompatibilities in initial conditions are rapidly "corrected" as the solutions evolve toward a cyclic behaviour. As noted in Table 2, the 14 cases studied have been equally divided between purely distended and collapsible tubes; the former with differing values of the wall compliance. The effect of reversed flow perfusion is examined for collapsible tubes, and discussed in the framework of published experimental results.

The graphs displayed in Figs. 12–17 have been plotted automatically in the computer. The left half portrays the pressure profiles in space and time as indicated by the three-dimensional surface plot, followed by three rows of $p-t$ curves; the first row corresponding to three equi-distant stations in the arterial portion of the lobe, the second to the entrance to the precapillaries, capillaries and exit from the post-capillary vessels respectively, while in the third row are represented profiles at three equi-distant stations in the venous portion. The bottom two curves represent, respectively, the proximal and distal boundary conditions on the pressure. In Figs. 12–14, this second curves reduces to the abscissa $p = 0$; whereas the distal pressure is maintained at a constant non-zero value (after an initial rapid ramp rise) for Figs. 15–17.

The right half of each figure depicts similar curves for the flow rate. Since each individual figure has been magnified to different degrees in order to fill its respective square, the scales may vary amongst them. Nonetheless, the following constant intervals (indicated on each coordinate axis) are common to all figures and are sufficient to quantify the graphical results: time interval 0.2 sec, pressure interval 2500 dyn/cm², and volume flow rate interval 25 cm³/sec. The boundary conditions will be chosen in order to permit direct comparison with the experimental

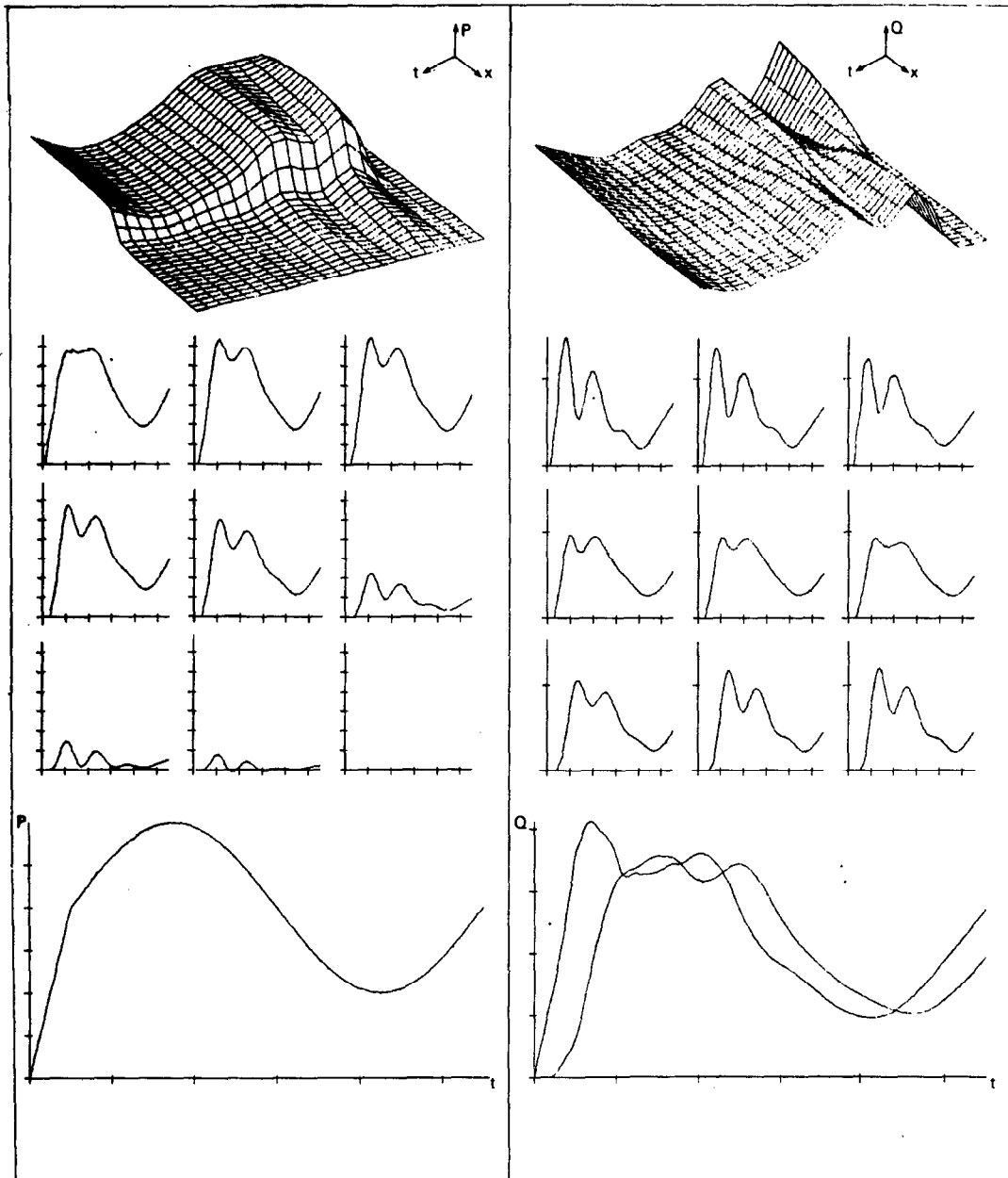


Fig. 12. Computed pulmonary pressure and flow fields, without collapse, at 1 Hz (case 2, Table 2).

results of Maloney *et al.* (1968).

Fig. 12 presents typical flow results for a 1 Hz input pressure variation of amplitude 5000 dyn/cm^2 superposed on a constant longitudinal pressure gradient corresponding to a pressure drop of $10,000 \text{ dyn/cm}^2$ ($10 \text{ cm H}_2\text{O}$) across the entire branched network. The computations clearly confirm the growth of the amplitude of pressure pulses in the arterial portion of the pulmonary circulation. Such behaviour has been observed experimentally in the systemic circulation, as

one moves progressively away from the heart. This amplification (cf. Attinger, 1963), quite contrary to the behaviour of rigid industrial branched conduit systems, has been largely attributed to the increase in wall stiffness with distance from the heart, as well as the nonlinear wave steepening character of the flow equations. The highly three-dimensional anatomy of the lung renders direct measurements (beyond the third generation of branching) extremely difficult, if not impossible, in the pulmonary circulation. For the

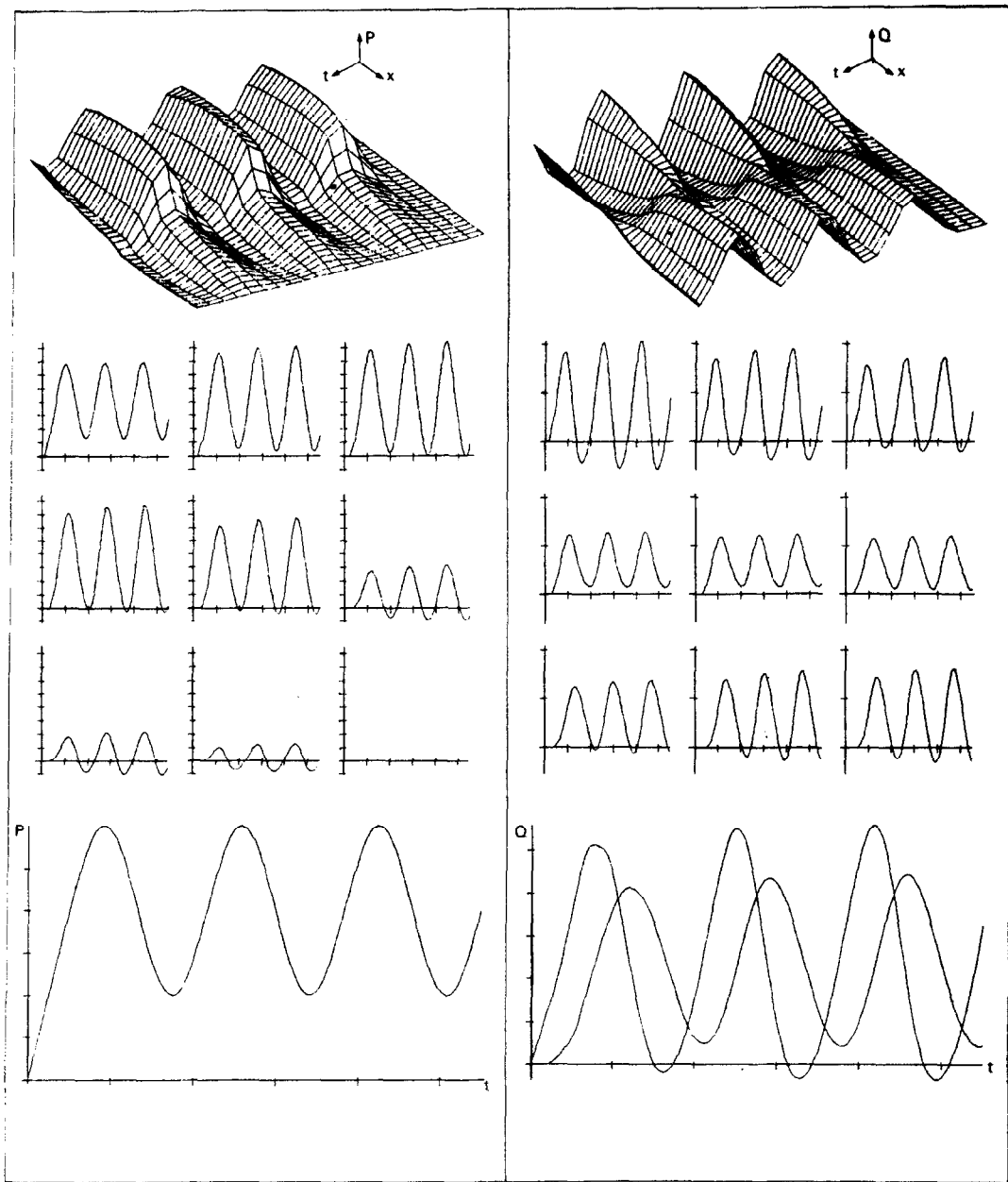


Fig. 13. Computed pulmonary pressure and flow fields, without collapse, at 3 Hz (case 4, Table 2).

intermediate flow field, one must rely upon realistic computations which account for a variation in vessel compliance as one progresses from the pulmonary artery toward the capillary bed. As was pointed out earlier, this variation is quite significant, resulting, in the present calculations, in differences in wave speed of a factor of five within the pulmonary circuit.

These results furthermore confirm the widely accepted hypothesis that the most significant portion of the pressure drop occurs in traversing the capillary bed.

The greatly attenuated pressure nonetheless still conserves its pulsatile character as it enters the pulmonary venous network: the abrupt drop in pressure at the capillary level is most striking in the three-dimensional surface plot of $p(x,t)$ in the top left corner of this sequence of figures.

The computed flow wave forms at the proximal and distal extremities (right-hand half of Fig. 12) indicate a time delay ($f = 3$ Hz) of approximately 0.1 sec for a flow disturbance to traverse the complete pulmonary

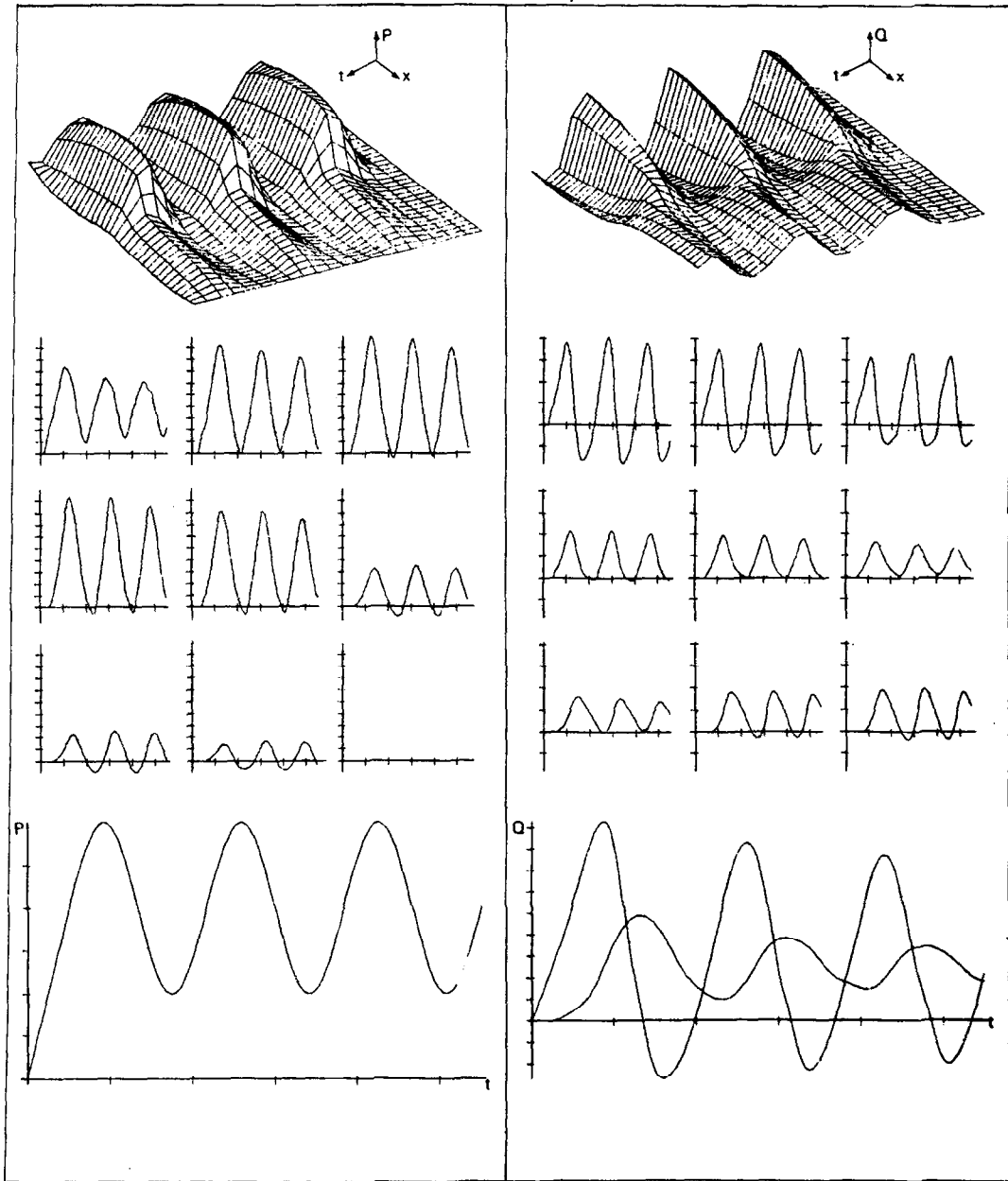


Fig. 14. Computed pulmonary pressure and flow fields, with doubled compliance, at 3 Hz (case 7, Table 2).

lobe, in agreement with Morkin *et al.* (1965). This also corresponds, for a transit distance of about 35 cm, to a velocity of 350 cm/sec, in excellent agreement with the measurements of Attinger (1963). In all figures for forward flow in the lung, the similarity between proximal pressure and flow-rate wave forms persists. This is not surprising, since in the absence of collapse (the onset of which is delayed at the proximal end where the transmural pressure is at its highest level), an elastic relation holds. However, the distal flow wave

forms become distorted in relation to the proximal wave shapes, due to the intervening regions of partial collapse and wave reflections. Flow oscillations are practically unattenuated in the pulmonary arterial system, but become partially damped as the blood enters the capillary bed. This behaviour is in complete qualitative agreement with the observations of Attinger (1963) for the inflated and deflated lung (cf. his Figs. 8 and 9 for pulmonary venous wedge pressure). The oscillations are again reinforced as the flow

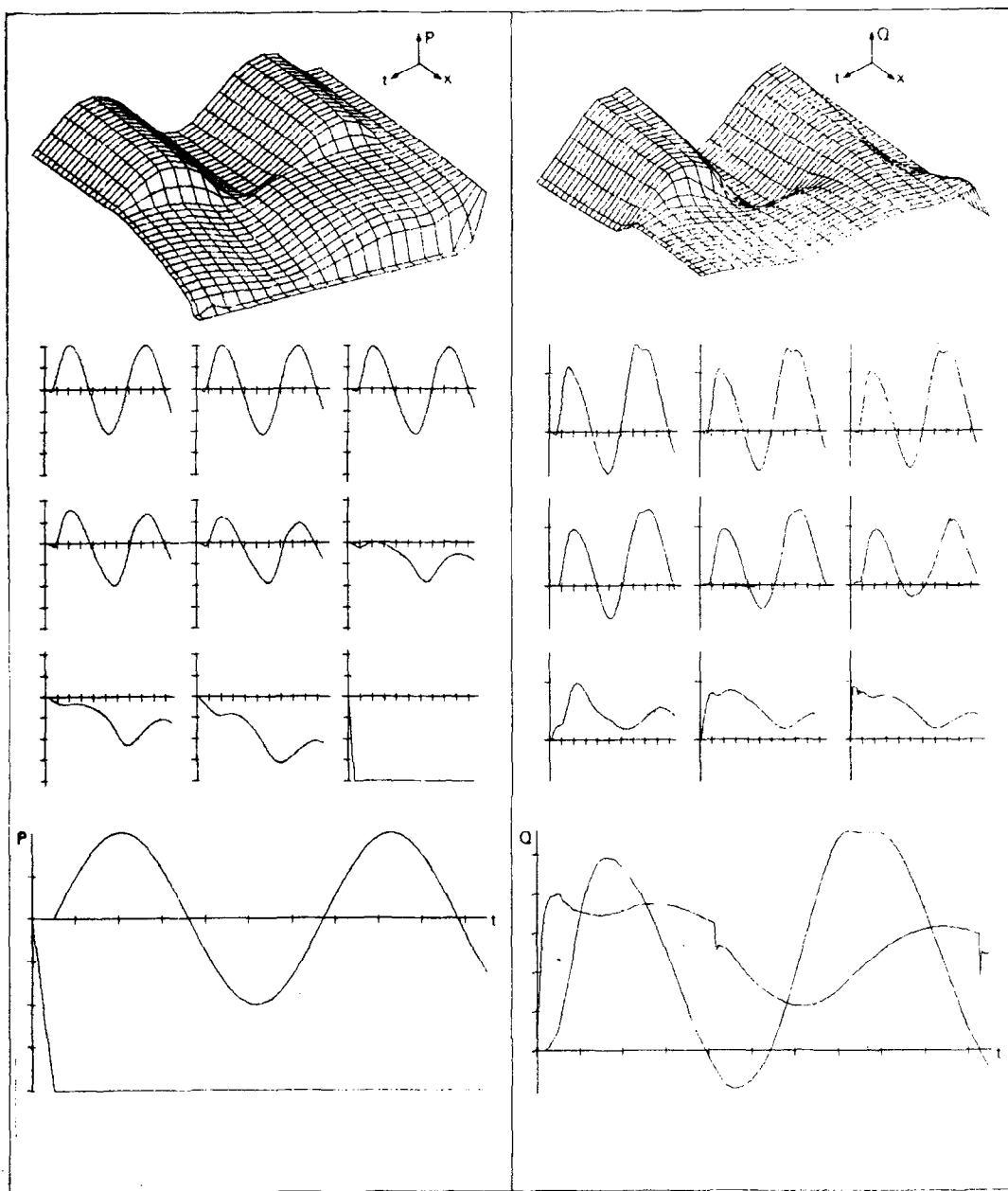


Fig. 15. Computed pulmonary pressure and flow fields, with collapse, at 1 Hz (case 9, Table 2).

emerges into the venous branching system.

Similar qualitative features of the flow are maintained as the frequency is increased. At 3 Hz (Fig. 13) the distal flow rate is seen to have fallen to about 70% of its proximal value (based on the ratio of the peak-to-peak amplitudes at the distal and proximal ends). In fact, this attenuation increases with increasing frequency, and has been confirmed experimentally by Maloney *et al.* (1968a, b). The flow transmission, defined by the distal/proximal ratios of the peak-to-peak amplitudes of the flow oscillations, has been

plotted for the combined cases 1-5 (Table 2) in Fig. 18a.

An important feature, which is most difficult to investigate in the laboratory, is the role played by wall compliance in the transmission of blood flow through the lung. Computational results (cases 6 and 7 of Table 2) have been obtained for one-half and for double the normal compliance. Curves for the latter case are shown in Fig. 14 and may be compared directly with the normal compliance results of Fig. 13 at the same frequency of 3 Hz. The effect is dramatic, as seen by the

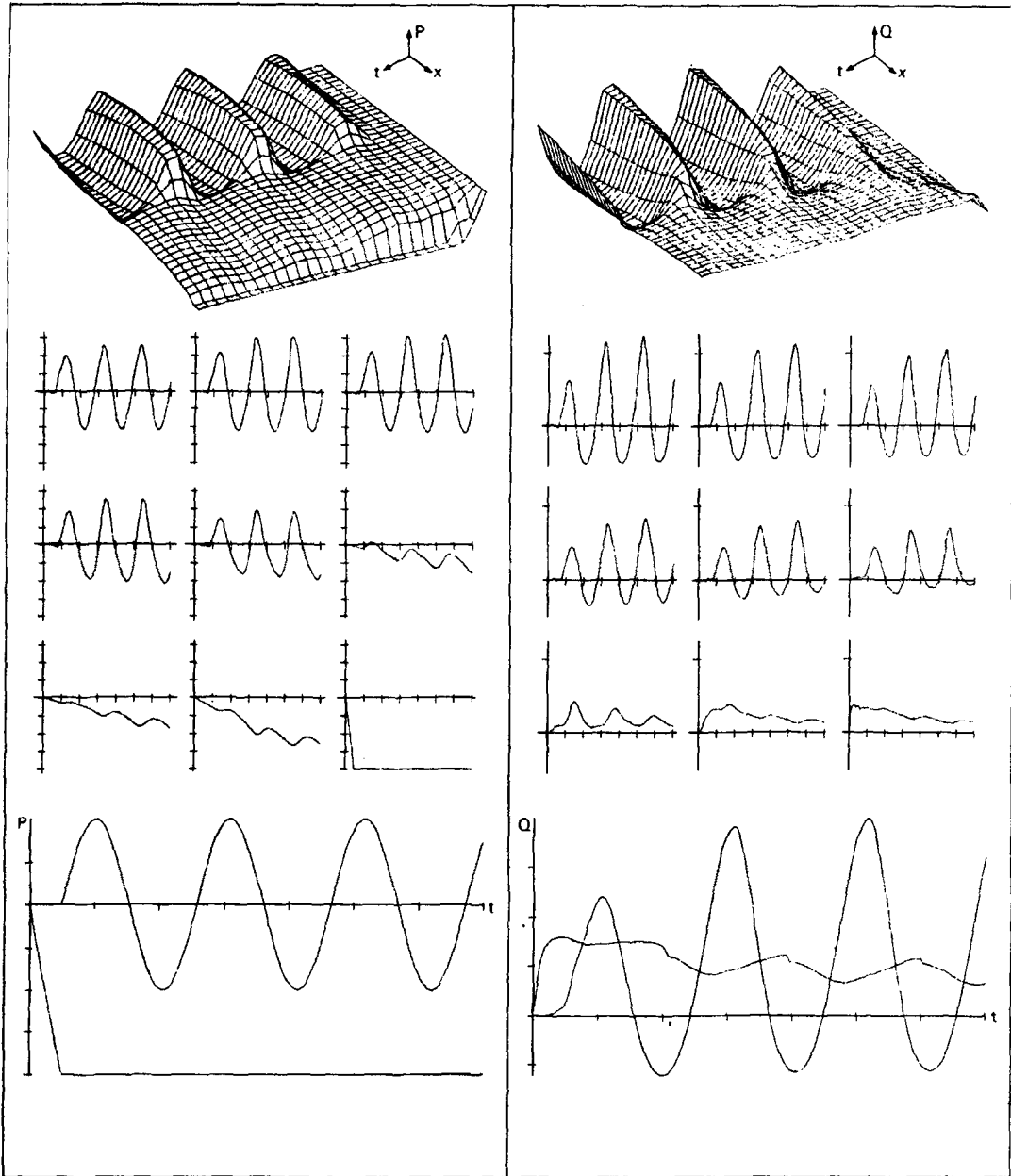


Fig. 16. Computed pulmonary pressure and flow fields, with collapse, at 3 Hz (case 11, Table 2).

very wide variation in flow transmission which results (Fig. 18b). Halving the compliance appears to render the vessels quasi-rigid, resulting in an almost 100% transmission of the blood flow from the pulmonary artery to the distal left atrium with virtually no losses (although viscous dissipation and a slight drop in stagnation pressure due to intermittent vortex formation at branch points may cause some attenuation). On the other hand, a general doubling of the vessel wall compliance leads to a marked drop in flow

transmission to a level of 20% as energy is dissipated in increased wall motion. (Attenuation in the localized capillary bed itself is, however, less affected by changes in compliance, since the natural pressure drop there is already much greater.)

But the effect of wall collapsibility will be seen to be even more significant! During collapse, the vessel momentarily assumes a high "effective compliance". Cases 8-11 (Table 2) have been computed with a provision for vessel collapse in a region extending from

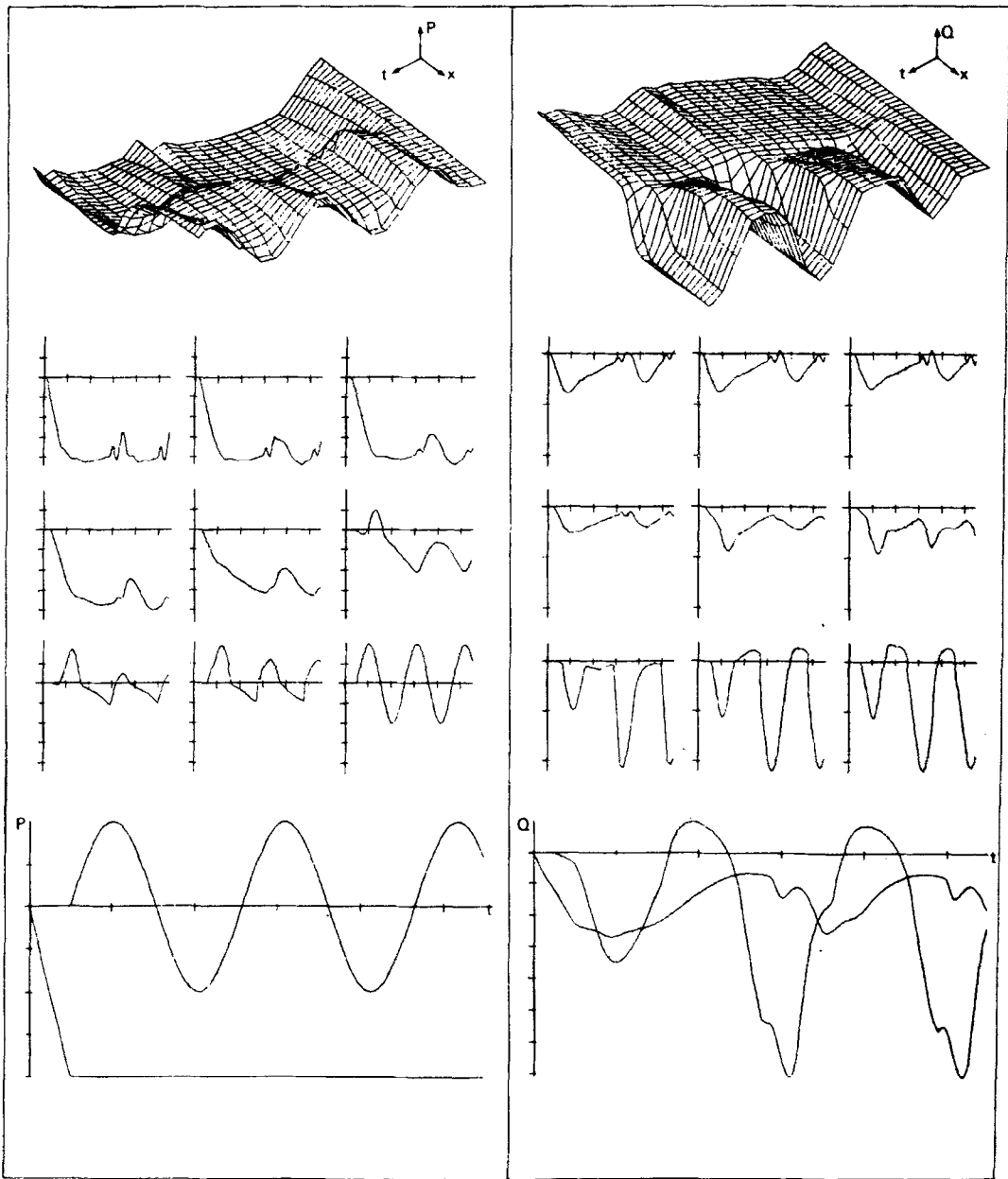


Fig. 17. Computed pulmonary pressure and flow fields, with retrograde flow at 3 Hz (case 13, Table 2).

the pre-capillaries to the left atrium for a range of pulsatile frequencies. Results of cases 9 (1 Hz) and 11 (3 Hz) are shown in Figs. 15 and 16, respectively. The proximal (pulmonary artery) transmural pressure was maintained at zero, upon which was superimposed a fluctuating sinusoidal component of amplitude 5000 dyn/cm^2 , while the distal end was maintained at a constant level of $-10,000 \text{ dyn/cm}^2$. Comparisons of Figs. 12 and 15 for a pulsatile flow at 1 Hz confirm that time-dependent pressure and flow oscillations are

smoothed out under conditions of partial collapse. The marked decrease in flow transmission for the collapsible network at 1 Hz is further corroborated in Figs. 14 and 15 for pulsatile flow at a frequency of 3 Hz. The results are general, and the variation of flow transmission with frequency for a collapsible pulmonary network is traced in Fig. 18(c), alongside the corresponding experimental results (Fig. 18d) of Maloney *et al.* (1968), which were carried out with boundary conditions corresponding to those utilized

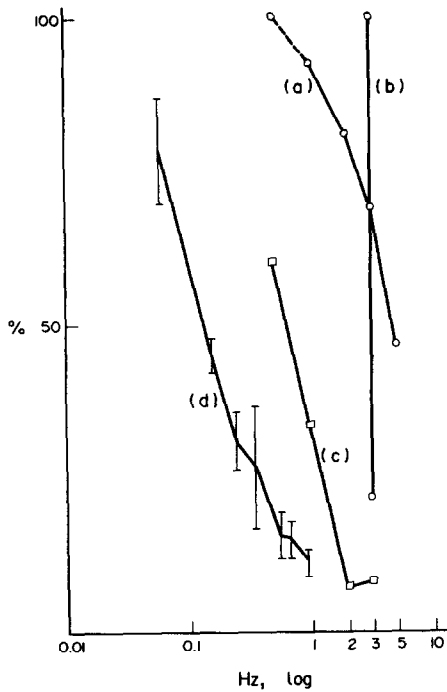


Fig. 18. Flow transmission in the lung as a function of pulsatile frequency:

- A: Computed without vessel collapse for normal wall compliance.
- B: Computed without vessel collapse for half and double compliances.
- C: Computed with vessel collapse and normal wall compliance.
- D: Measurements of Maloney *et al.* (1968b).

in the present numerical solution. Amongst the computed curves of flow transmission shown in Fig. 18, only the curve c which accounts for vessel collapse, adequately approaches the measured Maloney *et al.* (1968b) results. The comparison could probably be further improved by refining the model of tube collapse by means of a rigorous analysis of the dynamics of collapsible tubes (see for example Tedgui and Collins, 1978). The transmission curves for distensible vessels, without a provision for collapse (Fig. 18a), do not attenuate rapidly enough with increasing frequency. Although increases in wall compliance have been shown (Fig. 18b) to accelerate this attenuation, the magnitudes of compliance required are more than two-fold, and hence difficult to justify on purely physiological grounds. It would appear then that vessel collapse is an inherent and highly essential characteristic of pulsatile flow in the pulmonary circulation, and its role can be studied quantitatively. In fact, Maloney *et al.* (1968b) note that the net transmission of pulsatile flow in the lung is independent of outlet pressure. This is reminiscent of a global Starling resistor (Permutt *et al.*, 1962) for which the inlet minus external pressure difference regulates the outflow for vessels in a partially collapsed state.

If the transmural pressure is raised globally throughout the network (for example by deflating the lungs) one would intuitively expect the otherwise collapsed vessels to remain open during the flow cycle. Such an effect is indeed observed in the results of case 12 (Table 2) which resemble so closely those of case 2 (Fig. 12) that it has not been deemed necessary to reproduce them here. In effect, deflation of the lungs by 10 cm H₂O (10,000 dyn/cm²) "raises" the network out of the collapsible regime, and consequently places it on the slowly attenuated transmission curve of Fig. 18(a), corresponding to no collapse. In this case, time-dependent oscillations persist to a much greater extent than for the inflated lung (collapsible vessel) counterpart. This very phenomenon has been observed by Attinger (1963), who concludes from his experimental findings that "pulmonary capillary flow is less pulsatile during positive pressure inflation as compared to deflation".

Lastly, the present numerical solution may be employed to investigate the effect of retrograde flow on the transmission properties of the lung. Maloney *et al.* (1968b) conclude from their experiments that the transmission of pulsatile flow was identical for perfusion in the forward and reverse directions. This implies approximate symmetry of elastic properties in the arterial and venous segments of the lung, but these diverge as one moves away from the capillary bed (Table 1). This symmetry is also confirmed by Caro *et al.* (1965) in their experiments on the distensibility of blood vessels in isolated rabbit lungs. Maloney *et al.* (1968b) have measured identical values of compliance (0.5 ml/cm H₂O) in the arterial and venous segments of a horizontal isolated lung preparation.

The numerical results of case 13 (Fig. 17), utilizing the values of vessel compliance given by Wiener *et al.* (1966), appear to verify this conclusion when compared with Fig. 16 (case 11, Table 2) for forward flow at a frequency of 3 Hz in a collapsible network. In this respect, some qualifying observations should be made regarding the earlier studies of Caro *et al.* (1967) and the more recent model of Dawson *et al.* (1973).

Caro *et al.* (1967) studied pressure oscillations in patients without pulmonary hypertension. The authors observed higher attenuation of pressure transmission in the backward than forward flow direction, and attributed this effect to inequality of the arterial and venous compliances. It is possible however that some loss of control in the boundary conditions may have developed during their occlusion of the distal cross-section for purposes of measuring the "wedge" pressure oscillations. A similar comment is to be made concerning the studies of Maloney *et al.* (1968) using horizontal isolated lung preparations. Those authors explicitly point out their inability to maintain constant pressure at the downstream end of the pulmonary vessels. It is primarily for this reason that only their flow transmission data have been used in comparing predictions of the present mathematical solution. Qualitatively however, it is clear from the latter

experiments that pressure transmission is attenuated with increases in pulsatile frequency, in a manner similar to that of flow transmission.

Dawson *et al.* (1973) have presented a grossly-lumped model of the pulmonary vasculature consisting of collapsible parallel units, each made up of Starling resistors in series. They state that their numerical values were not chosen to correspond to physiological values, and that the simplified Starling resistor model "does not adequately handle the differences between forward and retrograde perfusion in the isolated lung" which their results would imply.

In view of these shortcomings, and the indications of the present analysis, there would appear to be no sound basis for concluding that forward and reverse pulmonary flows should be significantly different.

An interesting set of experiments aimed at determining the distribution of blood flow in a vertical lung and its variation with pulsatile frequency has been described by Maloney *et al.* (1968a). An isolated dog's lung was subjected successively to a pulsatile flow and pressure, at different frequencies between 0.03 and 2.3 Hz, superimposed on a steady-state level. The pulmonary blood flow was measured by a technique using injected radioactive xenon-133 which, due to its low solubility in blood, is convected into the alveoli as a gas, presumably in proportion to the local value of the blood flow rate. The investigators detected an augmentation of the flow about the height (h_m , say) in the lung at which they estimate that the pulmonary vessels are just on the verge of collapsing (i.e. local blood pressure equals alveolar pressure). This flow "excess" (relative to the flow level existing in the absence of the pulsatile component of the input flow and pressure) decays as one moves above and below the h_m level. Furthermore, the amplitude of this excess was found to decrease as the frequency increased up to 3 Hz. At these higher frequencies, the flow distribution was found to approach that of steady perfusion (with the exception of a localized region at the base of the lung in which this tendency was reversed).

Although we have not yet made a complete study of this phenomenon, the results of our cases 9 and 12 (Table 2) depicted in Figs. 15 and 13 respectively, presently permit a restricted basis of comparison. Only absolute values of the flow rate can be evaluated here, as no computations were made for the steady flow case which has no physiological significance. We recall that the only difference between the boundary conditions of cases 9 and 12 is that for the latter, the background pressure has been raised by the equivalent of about 10 cm H₂O. In other words, the results of case 12 (Fig. 12) can be taken to correspond to a horizontal section of lung lying 10 cm below that of case 9 (Fig. 15).

Under these conditions, it is noted that the upper section (Fig. 15) lies in a partially-collapsed state (corresponding to section D in Fig. 8 of Maloney *et al.*, 1968a). Back-flow occurs since the vessels in the capillary region have not fully collapsed. However, for the lower pulmonary section of our Fig. 12, the vessels

are fully open, and slightly distended. No backflow is evident here throughout the pulsatile cycle. (The situation may be likened to that of section F of Maloney *et al.*, Fig. 8.) The peak value of flow is the same in both our cases, under the influence of identical pressure gradients during the peak pressure phase.

It is clear that the net flow per cycle decreases in absolute value as one moves up a height of 10 cm between these two levels in the lung and approaches the collapsed state. This is indeed what one might intuitively expect. The point being made by Maloney *et al.* (1968a) is that in spite of this decrease in absolute flow level, an "excess" exists relative to the corresponding steady state. Their interesting thesis to explain this depends essentially upon the assumption that "in such a system no backflow will occur when the arterial pressure is less than the alveolar pressure, because the vessel will collapse".

In fact, the conditions necessary for vessel collapse are not so clear cut. A detailed analysis (Tedgui and Collins, 1978) of the dynamics of collapsible vessels shows that the conditions for collapse can be computed on the basis of the instantaneous cross-section, the local variation of longitudinal curvature of the vessel, and its residual tension, in addition to the temporal variation of transmural pressure. One may conclude from that investigation that pulmonary blood vessels may indeed fluctuate between a state of full distension and various degrees of partial collapse, without ever closing completely.

The "valvular mechanism" suggested by Maloney *et al.* (1968a) to explain flow excess, has intuitive appeal, but the highly complex and interactive nature of pulsatile flows through collapsible biological vessels subjected to longitudinal tension may call for some caution. The preliminary analysis developed here would appear to indicate that quantitative solutions are well within the realm of possible efficient computational procedures.

Finally, we note the influence of vessel collapse on the frequency at which maximum fluctuations in the flow rate occur. The maximum and minimum values of the flow rate at the inlet and outlet, respectively, of the pulmonary network appear in Fig. 19 as a function of pulsatile frequency. In the presence of vessel collapse, there is a marked resonance-like behaviour at a frequency of 2 Hz, very close to the natural cardiac frequency of the dog. If the provision for vessel collapse is suppressed in the model, these fluctuations appear to shift their maxima to a frequency of 3 Hz.

6. DISCUSSION

The foregoing results have confirmed that dynamic collapse of the pulmonary vessels is the key factor controlling the flow transmission characteristics in the lung. Its influence far outshadows variations produced by physiological changes in the blood viscosity, pressure gradient and overall wall elasticity.

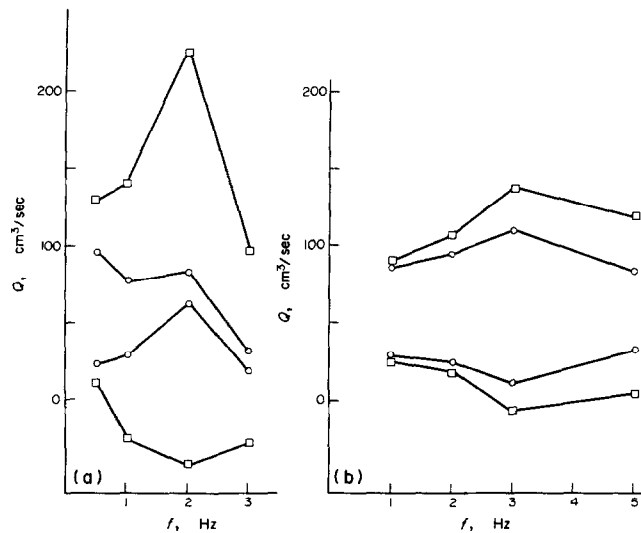


Fig. 19. Maximum and minimum values of flow rate Q at the inlet (□) and outlet (○) to the lung as a function of frequency for

- (a) collapsible pulmonary vessels
 (b) no provision for collapse.

In the interest of simplicity, only an approximate treatment of collapse has been suggested here. The principal feature of the present formulation hinges on the pre-assumed pressure–area law of Fig. 2.

This relationship incorporates the similarity analysis of Flaherty *et al.* (1972) which is valid in the region near complete collapse and has been verified by experiments (Shapiro, 1977) on thin-walled latex tubing. Its general configuration would be expected to conform reasonably well to the tube law for physiological vessels.

The slope of the linearized segments of the pressure–area curve (Fig. 2) represents the wall compliance, and is inversely proportional to the corresponding modulus of elasticity. The value of this compliance increases dramatically and abruptly as the initially distended vessel collapses, but the vessel subsequently re-assumes its lower compliance upon re-inflation. It is precisely this effective and sudden “switching” between high and low levels of “instantaneous elasticity” which has been shown here to account for the rapid decay in flow transmission observed by Maloney *et al.* (1968b). Permanently elevated values of compliance are neither effective nor realistic in explaining this attenuation with increasing frequency. Nor can the significant flow attenuation observed in the venous segments be well-reproduced in the computations without invoking vessel collapse. These results would tend to confirm the conclusions of Permutt and Riley (1963) on the relative importance of recruitment of collapsed vessels, as opposed to the further distension of open vessels.

6.1 Influence diagram

Drawing upon numerous sets of laboratory and clinical observations and measurements, it is useful to summarize pictorially, by means of an “influence diagram”, the system of causal relations linking the various physical parameters of the pulmonary circulation. Such an attempt is represented in Fig. 20, in which the arrows indicate the direction from cause to effect. Solid lines denote positive influences, i.e. changes in the cause and effect parameters have the same sign; whereas dashed lines denote negative influences, implying changes with opposite sign.

Most external influences are seen to act upon the pulmonary arterial pressure, which in turn controls the wall compliance via the position of the blood vessels in the pressure–area plane of Fig. 2. For example, on exercise, the pulmonary artery pressure increases (West *et al.*, 1964), thus opening (or recruiting) partially closed vessels. The flow field is displaced toward the right of Fig. 2 implying decreased values of the compliance ($\alpha \rightarrow \alpha_2$). Pressure and blood flow transmission are augmented, thus effectively enhancing the oxygenation capacity of the lung in the face of the external demand, by momentarily opening vessels normally in a partially collapsed state, and thereby extending the regions of effective blood perfusion and gas exchange within the lung. A similar response is elicited in the presence of a pulmonary occlusion or obstruction of the lumen, and the often associated condition of pulmonary hypertension. West *et al.* (1964) have pointed out that flow distribution in the lung can be completely accounted for by the mechani-

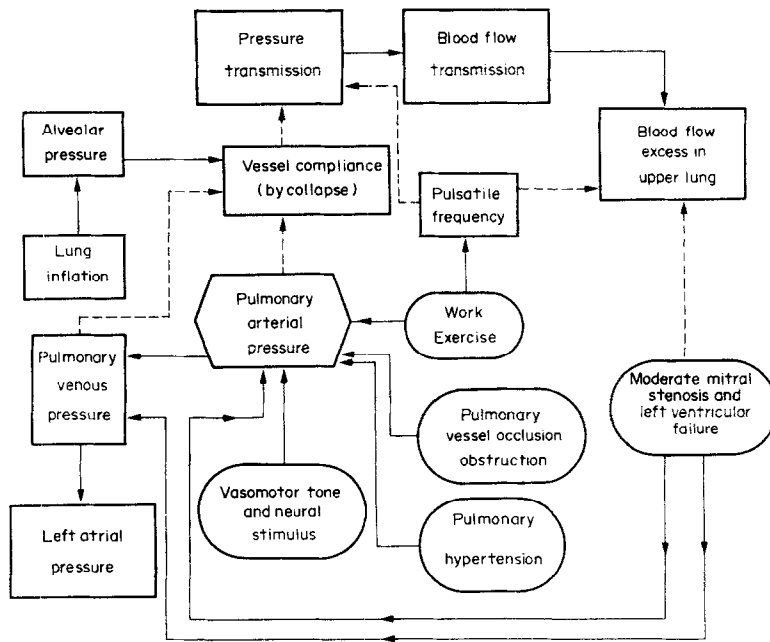


Fig. 20. Influence diagram for pulmonary response.

cal effects of transmural pressure. In this respect, neural control and vasomotor tone can be considered as acting directly upon the pulmonary arterial pressure, and hence mechanically upon the rest of the system, as depicted in Fig. 20. On the other hand, the predominant influence of mild mitral stenosis and left ventricular failure is to raise the pulmonary venous pressure, inducing a slighter rise in the pulmonary arterial pressure, which again shifts the system towards the right of the $S-p$ curve (Fig. 2), with the net effect of improving flow transmission, and perfusion of the upper portions of the lung. By such means, nature attempts to resist perturbations by returning the system to its normal state.

Maloney *et al.* (1968) report that, under certain conditions, transmission of pulsatile flow is independent of outlet pressure. The concept of a Starling resistor (Permutt *et al.* 1962) immediately comes to mind here. If the arterial pressure exceeds the alveolar pressure, which in turn is greater than the distal venous pressure, the flow is determined by the difference between the proximal arterial and external alveolar pressure, the venous pressure being likened to the bottom of a waterfall, clearly having no influence on the upstream conditions.

Milnor (1972), in his excellent review chapter on pulmonary hemodynamics, refers on page 325 to investigations showing that "resistance can be lowered by raising pulmonary arterial or venous pressures, but the mechanism for this effect is uncertain". However, a simple and rational explanation suggests itself on the basis of the foregoing influence diagram. If one interprets lowered "resistance" (a concept of very

limited utility which is associated with a mathematical similarity between the equations governing linearized fluid flow and an electrical transmission line) as equivalent to enhanced flow transmission, then the influence diagram (Fig. 20) shows immediately that increasing arterial pressure leads to a decrease in vessel compliance (by opening partially collapsed vessels - cf. Fig. 2) and an increase in pressure transmission and hence flow transmission, the latter implying a decreased "resistance".

Parenthetically, it is to be emphasised once again that a linearized flow analysis, along with its associated concepts of resistance or impedance, although in wide use by physiologists and clinicians, can miss some very important features of wave propagation in distensible tubes. Proper account of wave reflections at bifurcations and tube ends, and the progressive nonlinear steepening of pressure pulses in the arteries of both the systemic and pulmonary circulations, requires retaining the troublesome but important inertial terms in the governing equations of motion.

The present computational model should facilitate quantitative predictions of such pulmonary response. Nonetheless, certain features and limitations of the model bear further comment.

It has been found to be essential to include fluid viscosity, without which the numerical computations may become unstable. For simplicity, the capillary bed has been encompassed within the equivalent single conduit model, on the basis of vessel dimensions given by Wiener *et al.* (1966), notwithstanding the detailed "sheet-flow" model developed by Fung and Sobin (1969) for quasi-steady flow. The present results would

suggest that pulsatility persists down to the capillary level, an effect earlier corroborated by Skalak (1972). Although it may well be reasonable to describe capillary response as a succession of quasi-steady states as proposed by Fung *et al.* (1972), fluid acceleration cannot be neglected for most pulmonary vessels lying outside the capillary bed.

Non-stationary effects are clearly important in determining the pressure and flow fields, which appear to move in unison throughout the arterial segments of the pulmonary circulation. The calculations confirm the substantial pressure drop usually attributed to the capillary bed.

A certain number of secondary but interesting features which have not been included in this simplified analysis could easily be incorporated. One concerns the increase in entropy due to possible vortex formation at the dichotomous bifurcations within the 40-odd generation idealized pulmonary network. This is translated physically into a loss of stagnation pressure or "total head". Its effect in large vessels has been studied by Pedley *et al.* (1971) and others, and could easily be accounted for approximately in a one-dimensional flow model by adjusting the value of N in equation (3.5). Under normal physiological conditions, energy-dissipating vortices are rarely observed, and if so, are extremely short-lived as a result of the natural flow pulsatility.

The piecewise-linear pressure-area relation for the vessel wall (Fig. 2) can readily be generalized to curved segments with absolutely no additional computational difficulty. As indicated earlier, the data of Wiener *et al.* (1966) formed the basis of the examples computed here. More detailed information justifying a generalization of the tube law is not presently available. The far more important refinement lies in recognizing that such a pre-determined pressure-area relation does not rigorously exist *a priori*. Rather, the transmural pressure is a function not only of the local cross-sectional area, but also of the local radius of curvature in the longitudinal plane. Bergel (1972) notes that biological vessels are often under considerable residual axial tension, as they retract under excision from 25 to 40%.

The characteristics of such a vessel under conditions of dynamic collapse may be considerably modified by these restoring tensile forces, in the same way in which a guitar string vibrates in response to its pre-tension! The viscoelastic character of the vessel wall has been neglected here. On the basis of the experiments by Collins *et al.* (1978), one may safely discard viscoelastic forces in comparison with the above-mentioned constraints acting upon pulmonary vessels.

The present model may describe the type of horizontal lung preparation utilized in isolated lung experiments. Although the effect of gravity may be included in the fluid equations, good predictions for horizontal slices at different levels within the lung may be computed by adjustments of the pulmonary arterial and venous pressures to account for the variation in hydrostatic head.

7. CONCLUSIONS

A mechanical flow model of the complete pulmonary circulation has been formulated on the basis of the nonlinear unsteady equations of fluid motion. The introduction of an experimentally verified relationship between transmural pressure and local cross-sectional area, which provides for partial or total collapse of certain vessels, has been demonstrated to be an essential feature of the model. Good agreement has been obtained between predictions of sharp attenuation of flow transmission with pulsatile frequency and the experimental results reported by Maloney *et al.* (1968) for the isolated dog lung. It has been further shown that even substantial alterations in vessel wall rheology (compliance), without accounting for collapse, cannot produce this observed response.

The nonlinear features of the analysis are important for the proper treatment of wave reflections and the observed steepening of the pressure pulses in the proximal arterial segments of the pulmonary network. The model also predicts no significant differences in the character of forward and retrograde flows, in accordance with the consensus of experimental findings.

In the interest of simplicity, certain secondary effects, such as momentary losses in stagnation pressure due to possible short-lived bursts of vorticity at bends and branchings in the pulmonary tree during pulsatile flow, have not been included in this preliminary model. The influence of gravity is readily incorporated by adjustment of the pulmonary arterial pressure with height in the lung. Flow in the capillary bed has been treated simply by incorporating the vascular network within the 40-odd generations of the complete pulmonary tree. Computations confirm that the major drop in blood pressure occurs across the capillary bed.

The complex and controversial question of the existence of a spectrum of finite opening times for collapsible vessels (Maloney *et al.*, 1968a) is only partially answered by the present analysis. Its resolution hinges very sensitively on the form of the pressure-area law which one adopts. The present relation, which provides good phenomenological agreement with observed pulmonary behaviour, implies a dependence of vessel cross-section on local transmural pressure only. Therefore, changes in cross-sectional area are necessarily synchronous with pressure changes in this approximate formulation.

A definitive conclusion would require application of a simultaneous solution of the fluid and wall equations, without the assumption of such a pre-specified "tube law". An analysis of the dynamics of flow in collapsible tubes (Tedgui and Collins, 1978) proves considerably more complex as it accounts for the significant residual longitudinal tension and local curvature distribution of the vessel walls.

The pulmonary circulation appears to possess a self-regulating control system, whose character is

schematically represented here in the form of an influence diagram. It is suggested that mechanical (or even certain vasomotor) effects may act upon the pulmonary arterial pressure level which in turn regulates the instantaneous effective compliance of the collapsible vessel segments, thus determining the character of ensuing wave propagation. Such graphical representations of pulmonary response may eventually be quantified for specific clinical situations, hopefully providing an improved guide to correct diagnosis and therapy of pulmonary disorders.

REFERENCES

- Anliker, M., Rockwell, R. L. and Ogden, E. (1971) Nonlinear analysis of pulse waves and shock waves in arteries. *ZAMP* **22**, 217–246, 563–581.
- Attinger, E. O. (1963) Pressure transmission in pulmonary arteries related to frequency and geometry. *Circulation Res.* **12**, 623–641.
- Bergel, D. H. (1972) The properties of blood vessels. *Biomechanics, Its Foundations and Objectives*. (Edited by Fung, Y. C., Perrone, N. and Anliker, M.), p. 110. Prentice-Hall, Englewood Cliffs.
- Bruderman, I., Somers, K., Hamilton, W. K., Tooley, W. H. and Butler, J. (1964) Effect of surface tension on circulation in the excised lungs of dogs. *J. appl. Physiol.* **19**, 707–712.
- Caro, C. G., Harrison, G. K. and Mognoni, P. (1967) Pressure wave transmission in the human pulmonary circulation. *Cardiovasc. Res.* **1**, 91–100.
- Caro, C. G. and Saffman, P. G. (1965) Extensibility of blood vessels in isolated rabbit lungs. *J. Physiol.* **178**, 193–210.
- Collins, R. (1978) Blood flow in collapsible tubes. *S. Afr. mech. Engr* **28**, 138–142.
- Collins, R. and Kivity (1978) Dynamic rheology of viscoelastic tubes. *Biorheology* **15**, 173–179.
- Cumming, G., Harding, L. K., Horsfield, K., Prowse, K., Singhal, S. S. and Woldenberg, M. (1970) Morphological aspects of the pulmonary circulation and of the airways. *Fluid Dynamics of Blood Circulation and Respiratory Flow*. Agard Conf. Proc. **65**, 23–1.
- Cumming, G., Henderson, R., Horsfield, K. and Singhal, S. S. (1969) The functional morphology of the pulmonary circulation. *The Pulmonary Circulation and Interstitial Space* (Edited by Fishman, A. P. and Hecht, H. H.), University of Chicago Press, Chicago.
- Dawson, C. A., Jones, R. L. and Hamilton, L. H. (1973) A pulmonary circulation model based on forward and retrograde perfusion of isolated lungs. *J. appl. Physiol.* **35**, 103–110.
- Flaherty, J. E., Keller, J. B. and Rubinow, S. I. (1972) Post buckling behavior of elastic tubes and rings with opposite sides in contact. *SIAM J. appl. Math.* **23**, 446–455.
- Fung, Y. C. and Sobin, S. S. (1969) Theory of sheet flow in lung alveoli. *J. appl. Physiol.* **26**, 472–488.
- Fung, Y. C. and Sobin, S. S. (1972) Pulmonary alveolar blood flow. *Circulation Res.* **30**, 470–490.
- Kivity, Y. and Collins, R. (1974) Large amplitude wave propagation in arteries and veins. *Lecture Notes in Computer Science*. **11**, 213–239. Springer, Berlin.
- Maloney, J. E., Bergel, D. H., Glazier, J. B., Hughes, J. M. B. and West, J. B. (1968a) Effect of pulsatile pulmonary artery pressure on distribution of blood flow in isolated lung. *Resp. Physiol.* **4**, 154–167.
- Maloney, J. E., Bergel, D. H., Glazier, J. B., Hughes, J. M. B. and West, J. B. (1968b) Transmission of pulsatile blood pressure and flow through the isolated lung. *Circulation Res.* **23**, 11–24.
- Milnor, W. R. (1972) Pulmonary hemodynamics. *Cardiovascular Fluid Dynamics* (Edited by Bergel, D. H.), Vol. 2. 299–340. Academic Press, New York.
- Milnor, W. R., Conti, C. R., Lewis, K. B. and O'Rourke, M. F. (1969) Pulmonary arterial pulse wave velocity and impedance in man. *Circulation Res.* **25**, 637–649.
- Morkin, E., Collins, J. A., Goldman, H. S. and Fishman, A. P. (1965) Pattern of blood flow in the pulmonary veins of the dog. *J. appl. Physiol.* **20**, 1118–1128.
- Pedley, T. J., Schroter, R. C. and Sudlow, M. F. (1971) Flow and pressure drop in systems of repeatedly branching tubes. *J. Fluid Mech.* **46**, 365–383.
- Permutt, S., Bromberger-Barnea, B. and Bane, H. N. (1962) Alveolar pressure, pulmonary venous pressure and the vascular waterfall. *Med. Thoracalis* **19**, 239–260.
- Permutt, S., Caldini, P., Maseri, A., Palmer, W. H., Sasamori, T. and Zierler, K. (1969) Recruitment versus distensibility in the pulmonary vascular bed. *The Pulmonary Circulation and Interstitial Space*. (Edited by Fishman, A. P. and Hecht, H. H.). University of Chicago Press, Chicago.
- Permutt, S. and Riley, R. L. (1963) Hemodynamics of collapsible vessels with tone: the vascular waterfall. *J. appl. Physiol.* **18**, 924–932.
- Rideout, V. C. and Katra, J. A. (1969) Computer simulation study of the pulmonary circulation. *Simulation*. 239–245.
- Shapiro, A. H. (1977) Steady flow in collapsible tubes. *J. Biomech. Engrng* **99**, 126–147.
- Skalak, R. (1972) Mechanics of the microcirculation. *Biomechanics, Its Foundations and Objectives* (Edited by Fung, Y. C., Perrone, N. and Anliker, M.), p. 495. Prentice-Hall, Englewood Cliffs.
- Tedgui, A. and Collins, R. (1978) Unsteady flow in collapsible tubes. Submitted to *J. Fluid Mech.*
- Weibel, E. R. (1963) *Morphometry of the Human Lung*. Springer, Berlin.
- West, J. B., Dollery, C. T. and Naimark, A. (1964) Distribution of blood flow in isolated lung: relation to vascular and alveolar pressures. *J. appl. Physiol.* **19**, 713–724.
- Wiener, F., Morkin, E., Skalak, R. and Fishman, A. P. (1966) Wave propagation in the pulmonary circulation. *Circulation Res.* **19**, 834–850.